2020 IEEE International Conference on Robotics and Automation (ICRA)
31 May - 31 August, 2020. Paris, France

Internet of Things (IoT)-based Collaborative Control of a Redundant Manipulator for Teleoperated Minimally Invasive Surgeries

Hang Su[1], Salih Ertug Ovur[1], Zhijun Li[2], Yingbai Hu[3], Jiehao Li[1], Alois Knoll[3], Giancarlo Ferrigno[1] and Elena De Momi[1]

Abstract— **In this paper, an Internet of Things-based human-robot collaborative control scheme is developed in Robot-assisted Minimally Invasive Surgery scenario. A hierarchical operational space formulation is designed to exploit the redundancies of the 7-DoFs redundant manipulator to handle multiple operational tasks based on their priority levels, such as guaranteeing a remote center of motion constraint and avoiding collision with a swivel motion without influencing the undergoing surgical operation. Furthermore, the concept of the Internet of Robotic Things is exploited to facilitate the best action of the robot in human-robot interaction. Instead of utilizing compliant swivel motion, HTC VIVE PRO controllers, used as the Internet of Things technology, is adopted to detect the collision. A virtual force is applied to the robot elbow, enabling a smooth swivel motion for human-robot interaction. The effectiveness of the proposed strategy is validated using experiments performed on a patient phantom in a lab setup environment, with a KUKA LWR4+ slave robot and a SIGMA 7 master manipulator. By comparison with previous works, the results show improved performances in terms of the accuracy of the RCM constraint and surgical tip.**

I. INTRODUCTION

Robot-assisted minimally invasive surgery (RA-MIS), providing intuitive access to surgical operations, has garnered increasing research popularity in recent years because of its advantages compared to traditional open surgery, such as the reduction in recovery time, increased operational workspace and improved dexterity of the manipulation, etc. [1]. Nevertheless, due to the complexity under the kinematic constraint generated by the small incision point, RA-MIS requires expertise and continuous training for the surgeon [2], [3]. This small incision point on the abdominal wall, which has a diameter of less than an inch, is commonly known as the remote center of motion (RCM) constraint [4]. Hence, there are multiple tasks that, need to be handled together during the surgical operation in RA-MIS, such as the control of the surgical tip and the maintenance of the RCM constraint, which is unavoidable. Moreover, when there is a collision in the workspace, collision avoidance [5] without affects of the undergoing surgery is of vital importance for safety. Human-robot Interaction (HRI) has been one of the popular solutions to manage the workspace collision [6], [2]. Usually, the above multiple tasks are characterized by different priority levels [7]. For example, the general multiple tasks are listed as follows (T1–T3):

- i): The tracking control of the surgical tip must be accurate, which guarantees the success of the performed surgery using the robot manipulator [2].
- ii): The RCM kinematic constraint, produced by each small incision, should be respected [8].
- iii): Obstacle avoidance using HRI should be implemented to give the surgeon nearby access to a flexible workspace in the operating room [2], [3].

Hierarchical operational space proposed in [9], [10] is an efficient solution to achieve the multiple tasks controlled by the redundant serial manipulator. In our previous works [3], a control framework based on the hierarchical operational space was proposed to ensure T1–T3 together. It aims to limit the force exerted on the incision wall by the tool shaft, preventing patient injury.The collision can also be avoided using HRI with a compliant swivel motion strategy or using a remote body tracking system. However, a compliant swivel motion for HRI [6], which requires uncertain hands-on contact, leading to an error in the task space. The current remote body tracking system is not an optimal solution to predict human intention during the surgery in the complex environment of the operating room.

In recent years, the inspiration of devices communicating with each other has drastically increased. Communication between objects, makes the interaction with other objects such as sensing, identifying and networking, known as Internet of Things (IoT), possible [11], [12]. As a consequence of the infinite number of possibilities of interactions, IoT applications have spread widely to all research fields, and currently they have taken the lead in new research fields [13]. The Internet of Robotic Things (IoRT) is one application of IoT, which is widely used to address the integration of robotics technologies.

The role of robot-robot interaction and human-robot interaction [14] occupies an important place in the increasing research trend of IoRT. When IoRT supported robots are compared to stand-alone robots, IoRT benefits from sensing the presence of humans and allows human-robot interaction [13], [15]. In addition, the sensing capability, communication

*This work was supported in part by the European Commission Horizon 2020 research and innovation program, under the project SMARTsurg, grant agreement No. 732515 and in part by the Human Brain Project SGA2, under the Specific Grant Agreement No. 785907.

[1]Hang Su, Salih Ertug Ovur, Jiehao Li, Giancarlo Ferrigno and Elena De Momi are with the Department of Electronics, Information and Bioengineering, Politecnico di Milano, 20133, Milan, Italy. {hang.su, giancarlo.ferrigno,elena.demomi}@polimi.it {salihertug.ovur,jiehao.li}@mail.polimi.it

[2]Zhijun Li is with Department of Automation, University of Science and Technology of China, China. zjli@ieee.org

[3]Yingbai Hu and Alois Knoll are with the Department of Informatics, Technical University of Munich, Munich, 85748, Germany. yingbai.hu@tum.de; knoll@mytum.de

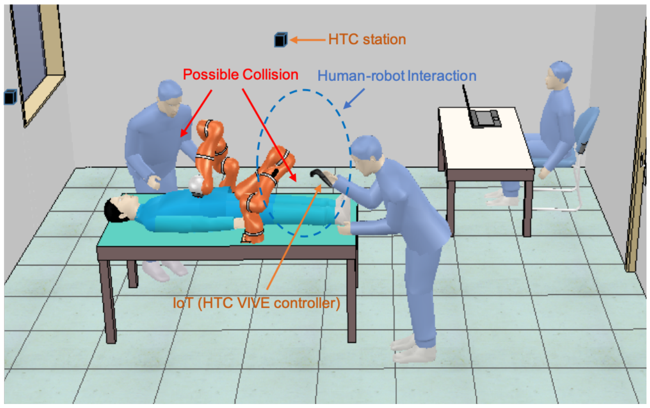

Fig. 1. Collision avoidance using IoT based Human-robot interaction.

through the internet makes human-robot interaction possible without physical interactions [16], providing improved control accuracy. Hence it is interesting to utilize the IoT based HRI to implement T3 without introducing uncertain hand contact force [17] during the control of the manipulator.

In this paper, an Internet of Things-based human-robot collaborative control scheme (IoTHRCC) is developed in a RA-MIS scenario. A hierarchical state equation is designed to exploit the redundancies of the 7-DoFs redundant robot to combine three tasks, T1, T2, and T3, simultaneously. Instead of utilizing compliant swivel motion, HTC VIVE PRO controllers used as an Internet of Things technology which is employed to measure the distance between the surgeon and robot. When there is a collision, a virtual force will be applied to the manipulator to move the robot elbow and spare a free workspace. The proposed IoTHRCC scheme avoids the direct hands-on contact of the surgical robot arm and utilizes a virtual force to move the swivel angle. In this case, compared with the solution proposed in [2], [3], the force applied to the robot arm is effective and provides a safer and more accurate solution.

II. RELATED WORKS

Prior works have been introduced to use redundant serial robot in Minimally Invasive Surgery. Sandoval *et al.* [4] proposed to exploit the redundancy to combine the T1 and the T2 at the same time, which involves an improved dynamic control method to apply the task redundancy for the RCM constraint (T2), without the influence of the surgical operation (T1). Sadeghian *et al.* [6] proposed a task-space control of robot manipulators (T1) with null-space compliance to avoid the collision in the workspace (T3). Few works have considered combining T1, T2 and T3. In our previous works [2], we solved T1 and T2 using tool pose trajectory planning and utilized the redundancy of the manipulator pose to achieve safety-enhanced compliant swivel motion (T3). Nevertheless, the T1 and T2 are not decoupled and the accuracy of the T1 is affected by the T2. Then in [3], we utilized the hierarchical operational space formulation [9] to combine three tasks T1, T2, and T3 in a hierarchical way without affecting each other.

In recent years, IoT has been more and more popular in robot applications with HRI, especially for collision avoidance. In [18], laser scanner and IMUs used for distance calculation for safer human-robot interaction. Safeea *et al.* [19] proposed an on-line collision avoidance for using IoT for collaborative robot manipulators by modifying off-line created paths using an industrial robot. They present a trend to utilize IoT techniques to avoid a collision without physical interaction.

III. METHODOLOGY

In this paper, we propose a novel method to utilize the benefits brought by IoT. The main contribution of this paper includes:

1) Introducing a novel swivel motion interaction control with IoT techniques to avoid direct hand contact on the robot body.
2) RBFNN is adopted to eliminate the uncertain disturbances existing in the system in a decouple way to improve the accuracy.
3) Experimental comparisons are performed with a hierarchical tasks scenario to demonstrate the effectiveness of the developed method.

As it is shown in Fig. 1, the HTC VIVE controller is used as IoT pre-calibrated with the robot system. In this way, there is real-time communication between the VIVE controller and the robot system. The distance between them can be calculated to detect a possible collision. If there is a collision in the workspace with the nearby surgeon in the operating room, a smooth virtual force will be applied to the robot manipulator to avoid the collision.

A. Teleoperation control of the Surgical tip

The surgical operation is controlled by the master manipulator through the vision interface. To drive the tool-tip position ($\boldsymbol{X} \in \mathbb{R}^3$) following the reference trajectory ($\boldsymbol{X_r} \in \mathbb{R}^3$) from the master, an interpolation method is implemented to allow the manipulator moving to the desired position ($\boldsymbol{X_d} \in \mathbb{R}^3$) efficiently:

$$\boldsymbol{X_d} = -k_0(\boldsymbol{X} - {}^s\boldsymbol{T}_m\boldsymbol{X}_r) + {}^s\boldsymbol{T}_m\dot{\boldsymbol{X}}_r \tag{1}$$

where ${}^s\boldsymbol{T_m}$ denotes the transformation matrix, and $k_0 > 0$ is a positive coefficient. Then a Cartesian compliance control term [4][2][20], $\boldsymbol{\tau_T}$, is proposed to perform impedance control of the surgical tip. The detailed implementation is shown in our previous works [2], [3]. For simplification, it is assumed that the desired trajectories are always within the reachable area, and the manipulator is far from its kinematic singularities.

B. Calibration of IoT with Robot for HRI

The HTC VIVE PRO controller has a reference frame, $\{v\}$, associated with respect to the HTC lighthouse base stations which is independently defined from the robot frame, $\{b\}$, shown in Fig. 2. Hence, registration is required between these two reference frames. To find a transformation matrix, calibration and validation steps are needed. In the calibration

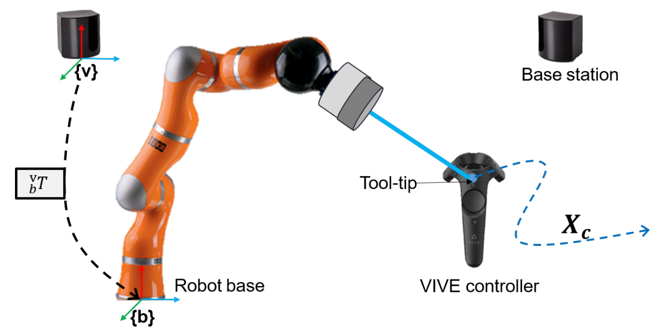

Fig. 2. Calibration of IoT in robot frame. $X_c \in \mathbb{R}^3$ is the performed calibration trajectory.

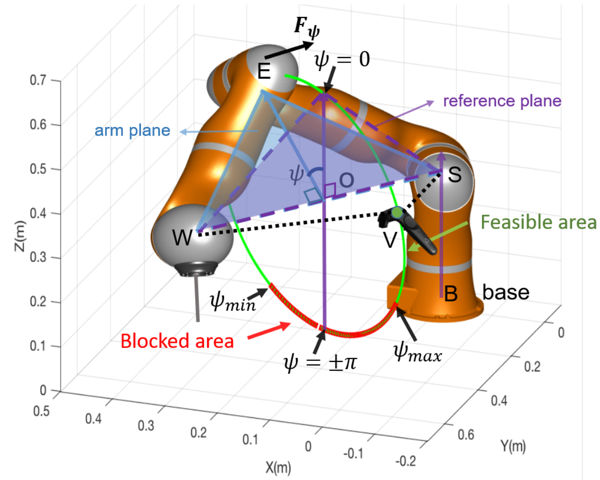

Fig. 3. Definition of the robot elbow swivel angle.

step, the tool-tip of the robot manipulator and the HTC VIVE PRO controller's origin are positioned at the same location for 5 seconds with 200 [Hz] sampling frequency for 15 different positions along a trajectory $\boldsymbol{X_c}$. Thanks to the Horn's quaternion-based method [21], the transformation matrix, ${}^{v}_{b}T$, between the two reference frames are computed. After the calibration has been done, transformation matrix ${}^{v}_{b}T$, is applied to the VIVE controller for validation. Three acquisition is performed by synchronous movement of the VIVE controller and robot tool in the space, with a duration of a minute under 200 Hz sampling frequency. The root-mean-squared error between the robot tool position and origin of the HTC VIVE PRO controller is computed as 1.7 [mm], 2.7 [mm] and 2.3[mm] for the three acquisitions, respectively. For these calculations, the KUKA robot is considered as a ground-truth. The results seem consistent with [22] which is claims a 2.63 [mm] trueness with respect to the CNC machine.

C. IoT based human-robot collaborative control

1) Swivel motion definition: As mentioned in our previous works [2], [3], due to the kinematic redundancy of the manipulator, a swivel motion with the robot elbow can be performed without moving the robot tool pose. The angle, ψ, between the robot arm reference plane (BSW) and the actual arm plane (SEW), is called swivel angle, shown in Fig. 3. It can be obtained by:

$$\psi = sgn((\vec{BS} \times \vec{SE}) \cdot \vec{SW}) \arccos\left(\frac{(\vec{BS} \times \vec{SW})(\vec{SE} \times \vec{EW})}{||\vec{BS} \times \vec{SW}||||\vec{SE} \times \vec{EW}||}\right) \tag{2}$$

where ($\vec{BS}$, $\vec{SE}$, $\vec{SW}$, $\vec{EW}$) denote the vector from base to the shoulder, the shoulder to the elbow, the shoulder to the wrist, and the elbow to the wrist, respectively. The full swivel motion range is $[-\pi, \pi]$. Due to the kinematic limitations, it is divided into a feasible area $[\psi_{min}, \psi_{max}]$ and two blocked areas $[-\pi, \psi_{min})$ and $(\psi_{max}, \pi]$ [23].

Except for the swivel angle ψ of the robot manipulator, to measure the distance between the robot elbow and the possible collision in the workspace, the swivel angle of VIVE controller, ψ_V, between the reference plane (BSW) and the VIVE plane (SVW), is defined:

$$\psi_V = sgn((\vec{BS} \times \vec{SE}) \cdot \vec{SW}) \arccos\left(\frac{(\vec{BS} \times \vec{SW})(\vec{SV} \times \vec{VW})}{||\vec{BS} \times \vec{SW}||||\vec{SV} \times \vec{VW}||}\right) \tag{3}$$

2) IoT-based swivel motion control: After the definition of the robot swivel angle, ψ, and the VIVE swivel angle, ψ_V, an IoT-based swivel motion control approach is proposed to obtain the desired swivel angle ψ_d. Considering the safety, we use the button on VIVE controller to switch on or off the swivel motion control. Hence, the control mode is working incrementally.

- When the button is pushed, the swivel motion control is activated and ψ_{init} is the initial swivel angle at the starting time t_{init}. The swivel motion of the manipulator is guided by the VIVE controller:

$$\psi_d = \psi_{init} + \xi \int_{t_{init}}^{t_{curr}} \dot{\psi}_V dt \tag{4}$$

  where $\dot{\psi}_V \in \mathbb{R}$ is the velocity of the VIVE swivel motion. $\xi \in \mathbb{R}$ is a positive scaling coefficient and t_{curr} is the current time.
- When the button is off, the swivel motion control is off. The compliant arm behaviour will be activated. Hence,

$$\psi_d = \psi \tag{5}$$

To drive the swivel motion following ψ_d in the pre-defined safe area, $[\psi_{minf}, \psi_{maxf}]$, a virtual force $\mathbf{F}_\psi = \mathbf{u}_{\mathbf{F}_\psi} \cdot ||\mathbf{F}_\psi||$ will be applied to the robot manipulator to enable the swivel motion. $\mathbf{u}_{\mathbf{F}_\psi}$ is the force direction vector, which is perpendicular to the BSW plane, defined as:

$$\mathbf{u}_{\mathbf{F}_\psi} = sgn(\psi_d - \psi) \cdot \frac{\vec{\mathbf{SE}} \times \vec{\mathbf{EW}}}{||\vec{\mathbf{SE}} \times \vec{\mathbf{EW}}||} \tag{6}$$

To achieve smooth swivel motion, an interpolation method proposed in the related work [2] is introduced to obtain the smooth control input $\bar{\psi}_d$. The virtual force F_ψ can be expressed as:

$$\mathbf{F}_{\psi} = \begin{cases} \mathbf{u}_{\mathbf{F}_{\psi}} \cdot (k_{\psi}(\psi_{minf} + \rho - \psi) - d_{\psi}\dot{\psi}) & \psi < \psi_{minf} \\ \mathbf{u}_{\mathbf{F}_{\psi}} \cdot (k_{\psi}(\psi_{maxf} - \rho - \psi) - d_{\psi}\dot{\psi}) & \psi > \psi_{maxf} \\ \mathbf{u}_{\mathbf{F}_{\psi}} \cdot (k_{\psi}(\psi_{d} - \psi) - d_{\psi}\dot{\psi}) & [\psi_{minf}, \psi_{maxf}] \end{cases}$$

where k_{ψ} and d_{ψ} are the constant coefficients. $\rho \in R$ denotes a positive constant threshold state of the swivel constraint.

3) Adaptive compensation: Since there is a physical interaction between the patient's abdominal wall and on the small incision the surgical tool shaft, it generates an external disturbance $\boldsymbol{F_e}$ on the tool shaft, which is unknown and nonlinear.The precision of the surgical tip and the RCM constraint can be limited by the disturbances. We plan to introduce a RBFNN [24] based decoupled approximation to improve the accuracy of the surgical tool-tip and maintain the RCM constraint.

Thus, the input Z of RBFNN is chosen with the actual Cartesian position $\boldsymbol{X}$ and the RCM constraint distance d. The uncertain disturbance $\boldsymbol{F}(\boldsymbol{X}, \dot{\boldsymbol{X}}, \boldsymbol{d}, \dot{\boldsymbol{d}})$ is represented as:

$$\boldsymbol{F}(\boldsymbol{X}, \dot{\boldsymbol{X}}, \boldsymbol{d}, \dot{\boldsymbol{d}}) = \boldsymbol{\Theta} \cdot \boldsymbol{\xi}(\boldsymbol{X}, \dot{\boldsymbol{X}}, \boldsymbol{d}, \dot{\boldsymbol{d}}) + \varepsilon \tag{7}$$

where ε is the smallest approximation error of RBFNN algorithm, $\boldsymbol{\Theta} = [\theta_1, \theta_2, ..., \theta_l]^T$ is the optimal constant weight matrix of neural networks, l is the number of nodes used in neural networks, and $\boldsymbol{\xi}(\boldsymbol{X}, \dot{\boldsymbol{X}}, \boldsymbol{d}, \dot{\boldsymbol{d}}) = [\xi_1, \xi_2, ..., \xi_l]$ is Gaussian function matrix. According to the theory of RBFNN, it can be addressed the upper bound of the approximation error ε^*, i.e., $|\varepsilon| \leq \varepsilon^*$, under a positive constant $\varepsilon^* > 0$.

The Gaussian function matrix used in the RBFNN algorithm can be represented as follows:

$$\xi_i(Z) = \exp\left[\frac{-(Z - c_i)^T (Z - c_i)}{b_i^2}\right] \tag{8}$$

where (b_i, c_i) denote the width of the Gaussian function and the center of the receptive field, respectively. According to the approximation rule, a positive constant can be constrained as follows: δ subjected to $\|\xi(Z)\| \leq \delta$ with $\delta > 0$.

The adaptive neural network updating law [24] is introduced to adjust the weights of neural network as:

$$\dot{\boldsymbol{\Theta}} = \boldsymbol{\gamma}[\boldsymbol{E}\boldsymbol{\xi}^T(\boldsymbol{X}, \dot{\boldsymbol{X}}, d, \dot{d}) + \boldsymbol{\varsigma}\boldsymbol{\Theta}] \tag{9}$$

where $\boldsymbol{\gamma}$ is a diagonal positive definite constant matrix determining the updating speed, $\boldsymbol{E} = [\boldsymbol{X_d} - \boldsymbol{X}, d]^T$, and ς is a momentum factor matrix of neural networks, which can improve both training speed and accuracy.

In order to compensate for the uncertainties in physical interaction, an adaptive neural network compensator is designed as:

$$\boldsymbol{\tau}_{T_2} = \boldsymbol{J_T}\boldsymbol{\Theta}^T\boldsymbol{\xi}(\boldsymbol{X}) \tag{10}$$

$$\boldsymbol{\tau}_{N_{12}} = (\boldsymbol{I} - \boldsymbol{J}_T^T(\boldsymbol{q})\boldsymbol{J}_T(\boldsymbol{q})_M^{+})\boldsymbol{J}_W\boldsymbol{\Theta}^T\boldsymbol{\xi}(d)\boldsymbol{F}_N \tag{11}$$

where $(\boldsymbol{J_T}, \boldsymbol{J_w})$ denote the end effector Jacobian matrix and the wrist joint Jacobian matrix, respectively. Then the implemented hierarchical control framework proposed in [3] will be utilized to handle the multiple tasks. Finally, the optimized control term can be expressed as:

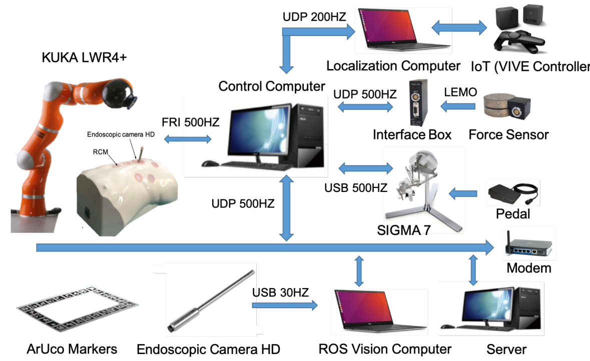

Fig. 4. Overview of the developed surgical robot system.

$$\boldsymbol{\tau_d} = \boldsymbol{\tau}_{T_1} + \boldsymbol{\tau}_{T_2} + \boldsymbol{\tau}_{N_{11}} + \boldsymbol{\tau}_{N_{12}} + \boldsymbol{\tau}_{N_2} \tag{12}$$

where $\boldsymbol{\tau}_{T_1}$ is the task space control term. $\boldsymbol{\tau}_{N_{11}}$ is the RCM control term. $\boldsymbol{\tau}_{N_2}$ is the control term for swivel motion control. The detailed definition and expression can be found in our previous works [3].

IV. SYSTEM DESCRIPTION

Elements of the teleoperated MIS system is shown in Fig. 4. The system is comprised of:

- A serial redundant robot (LWR4+, KUKA, Germany) is used to provide a direct low-level real-time access to the robot controller using the Fast Research Interface (FRI) [25];
- To implement a 3D Cartesian incremental teleoperation control, the haptic device (Sigma 7, Force Dimension, Switzerland) is used for the application;
- An HD endoscopic camera and an ArUco marker board [26], that are used for virtual surgical task tracking in an augmented reality environment;
- A 6-axis force sensor (M8128C6, SRI, China), used to measure the interaction force between the abdominal wall and the surgical tip.
- A HTC VIVE PRO full kit including the wireless HTC VIVE PRO Joystick and two HTC lighthouse base stations adopted to serve as an IoT for the localization of the motion of the surgeon.

The control system has been developed using two separate computers communicating through an UDP protocol. The first one, the "control computer", executes the real-time control loops implemented using OROCOS[1], with a real-time Xenomai-patched Linux kernel. The second one, the "vision computer", runs the perception algorithms developed using ROS[2] Kinetic under Ubuntu.

V. EXPERIMENTAL DEMONSTRATION

The experiments set up procedure is presented in Fig. 5. To validate the proposed IoTHRCC approach, we perform

[1]Open Robotic Control Software, http://www.orocos.org/
[2]Robot Operating System, http://www.ros.org/

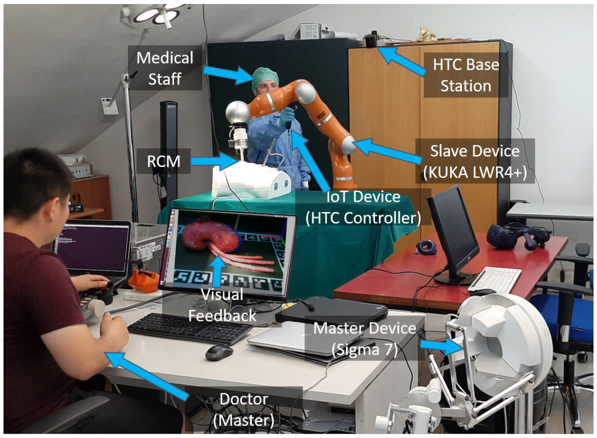

Fig. 5. Experimental setup scenario.

TABLE I
EXPERIMENTAL CONTROLLER PARAMETERS

Controller	Controller parameters
$\tau_d = \tau_{T_1} + \tau_{N_{11}} + \tau_{T_2} + \tau_{N_{12}} + \tau_{N_2}$	$\boldsymbol{K_X} = diag[3000, 3000, 3000]$ $\mathbf{D_X} = diag[30, 30, 30]$ $\boldsymbol{K_N} = diag[800, 800, 800]$, $k_0 = 0.1$ $\boldsymbol{D_N} = diag[10, 10, 10], k_\psi = 200, d_\psi = 2$ $\lambda = 0.5, b = diag[2, 2, 2, 2, 2]$ $\boldsymbol{\gamma} = diag[1.5, 1.5, 1.5, 0.5]$ $\boldsymbol{\varsigma} = diag[0.13, 0.13, 0.13, 0.03]$ $\boldsymbol{c} = diag[-3.0, -1.5, 0, 1.5, 3.0, 3.5]$

experiments in the laboratory setup environment employing a patient phantom. The RCM constraint is validated with physical interaction. And the surgical tip is teleoperated to track virtual trajectories without physical interaction. One teleoperator (User 2) and one surgeon (User 1) were enrolled. Hands-on control is performed to allow the user 1 locating the RCM constraint and insert the surgical tool into the patient phantom. Then teleoperation mode is activated to track the surgical tasks in augmented reality by User 2. The teleoperation tracking of three different tracking tasks in augmented reality is repeated 5 times each. At the same time, the robot arm is moved by user 1 using VIVE controller in an allowed swivel motion area [2], [3]. Table I presents the corresponding control parameters.

We experimentally demonstrate the concept of IoTHRCC and compared its performance with improved human-robot collaborative control (IHRCC) [3]. It should be mentioned that IHRCC handles the disturbances using fuzzy approximation, while RBFNN is used for the nonlinear approximation in IoTHRCC. The previous work manages collision avoidance with direct hand contact, and the novel one proposes a touchless solution. The measured Cartesian position error, $\boldsymbol{E_X}$, the RCM constraint error, d, and the interaction force $\boldsymbol{F_e}$ [3], [27]. The force sensor has been pre-calibrated in our previous works [27]. This procedure is only validated when the surgical tip travels in free space within the abdominal cavity, which means there are no contact forces at the instrument tip.

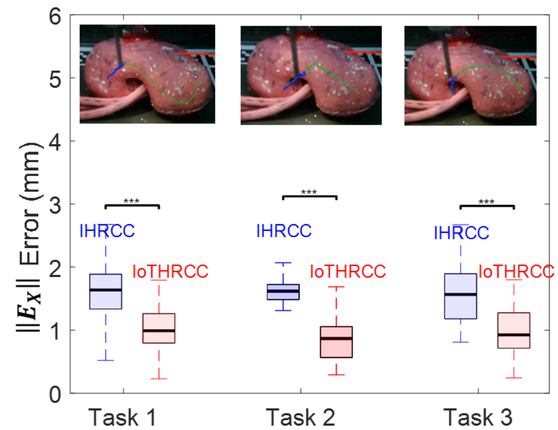

(a) Distribution of end-effector error $\|\boldsymbol{E_X}\|$

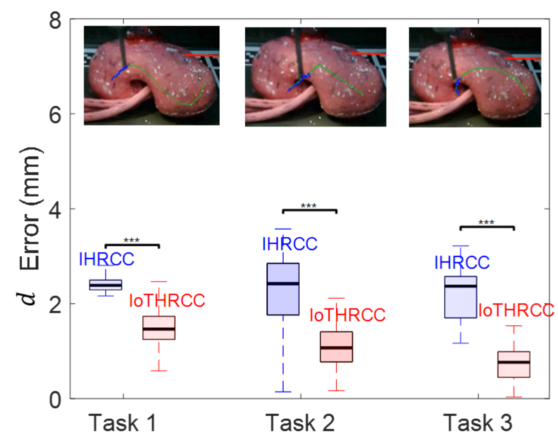

(b) Distribution of RCM constraint error d

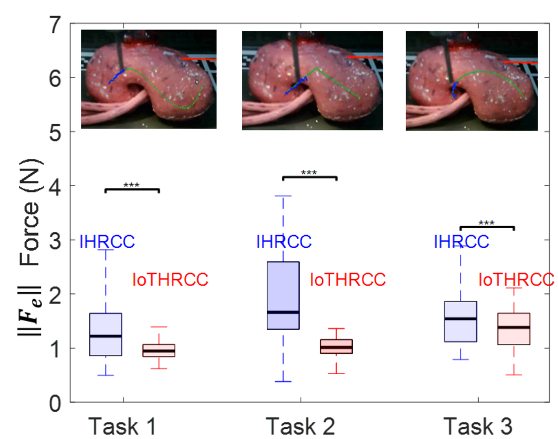

(c) Distribution of interaction force $\|\boldsymbol{F_e}\|$ on the RCM constraint

Fig. 6. Comparison between DCAC and IHRCC. Statistical significance (evaluated with one way-ANOVAs and post-hoc tests) is indicated with lines and stars(* for p<0.05, ** for p<0.01, *** for p<0.001)

It should be noticed that the swivel motion affects the tracking performance and the RCM constraint error.The corresponding distribution of the error of the surgical tip, $\boldsymbol{E_X}$, is shown in Fig. 6(a). Fig. 6(b) depicts the corresponding distribution of RCM constraint error d. The corresponding distribution of interaction force $||\boldsymbol{F_e}||$ on the small incision during the teleoperation tracking is presented in Fig. 6(c). Compared with IHRCC, direct hand contact on the robot is avoided, and the accuracy of the surgical tip is improved. Meanwhile, the error of the RCM constraint and the interaction forces are converged into a smaller scale.

VI. DISCUSSION AND CONCLUSION

An Internet of Things-based human-robot collaborative control scheme (IoTHRCC) is introduced for Robot-assisted Minimally Invasive Surgeries. The concept of the Internet of Robotic Things is introduced to facilitate the best action of the robot in Human-robot interaction. Instead of utilizing compliant swivel motion, the HTC Vive Pro interface is employed as a contactless approach to detect the collision and control the swivel motion. It is for the further development of the control scheme in order to consider the challenges associated with IoT technologies. A virtual force is applied to the robot elbow, enabling a safe swivel motion for Human-robot interaction. The effectiveness of the proposed strategy is demonstrated using experiments performed on a patient phantom in a lab setup environment. By comparison, the results show improved performances in terms of the accuracy, both for the RCM constraint and the surgical tip. Compared to the improved human-robot collaborative control in [3], hand contact is avoided and the accuracy is improved. It shows that the interaction between IoT and the robot produces a weaker influence on the teleoperation transparency and stability of the system compared to the compliance collision behavior with hand contacts.

REFERENCES

[1] A. M. Okamura, C. Simone, and M. D. O'leary, "Force modeling for needle insertion into soft tissue," *IEEE transactions on biomedical engineering*, vol. 51, no. 10, pp. 1707–1716, 2004.

[2] H. Su, J. Sandoval, M. R. Makhdoomi, G. Ferrigno, and E. De Momi, "Safety-enhanced human-robot interaction control of redundant robot for teleoperated minimally invasive surgery," in *International Conference on Robotics and Automation*, 2018, pp. 6611–6616.

[3] H. Su, C. Yang, G. Ferrigno, and E. De Momi, "Improved human–robot collaborative control of redundant robot for teleoperated minimally invasive surgery," *IEEE Robotics and Automation Letters*, vol. 4, no. 2, pp. 1447–1453, 2019.

[4] J. Sandoval, H. Su, P. Vieyres, G. Poisson, G. Ferrigno, and E. De Momi, "Collaborative framework for robot-assisted minimally invasive surgery using a 7-dof anthropomorphic robot," *Robotics and Autonomous Systems*, vol. 106, pp. 95–106, 2018.

[5] A. M. Zanchettin, N. M. Ceriani, P. Rocco, H. Ding, and B. Matthias, "Safety in human-robot collaborative manufacturing environments: Metrics and control," *IEEE Transactions on Automation Science and Engineering*, vol. 13, no. 2, pp. 882–893, 2015.

[6] H. Sadeghian, L. Villani, M. Keshmiri, and B. Siciliano, "Task-space control of robot manipulators with null-space compliance," *IEEE Transactions on Robotics*, vol. 30, no. 2, pp. 493–506, 2014.

[7] H. Su, S. Li, J. Manivannan, L. Bascetta, G. Ferrigno, and E. D. Momi, "Manipulability optimization control of a serial redundant robot for robot-assisted minimally invasive surgery," in *2019 International Conference on Robotics and Automation (ICRA)*, May 2019, pp. 1323–1328.

[8] N. Aghakhani, M. Geravand, N. Shahriari, M. Vendittelli, and G. Oriolo, "Task control with remote center of motion constraint for minimally invasive robotic surgery," in *Robotics and Automation (ICRA), 2013 IEEE International Conference on*. IEEE, 2013, pp. 5807–5812.

[9] A. Dietrich, C. Ott, and J. Park, "The hierarchical operational space formulation: Stability analysis for the regulation case," *IEEE Robotics and Automation Letters*, vol. 3, no. 2, pp. 1120–1127, 2018.

[10] K. Bussmann, A. Dietrich, and C. Ott, "Whole-body impedance control for a planetary rover with robotic arm: Theory, control design, and experimental validation," in *2018 IEEE International Conference on Robotics and Automation (ICRA)*, May 2018, pp. 910–917. [Online]. Available: https://ieeexplore.ieee.org/abstract/document/8460533

[11] A. Čolaković and M. Hadzialic, "Internet of things (iot): A review of enabling technologies, challenges, and open research issues," *Computer Networks*, vol. 144, 07 2018.

[12] R. Batth, A. Nayyar, and A. Nagpal, "Internet of robotic things: Driving intelligent robotics of future - concept, architecture, applications and technologies," 08 2018, pp. 151–160.

[13] B.-T. Akimana, M. Bonnaerens, J. Van Wilder, and B. Vuylsteker, "A survey of human-robot interaction in the internet of things," 12 2016.

[14] A. Ajoudani, N. Tsagarakis, and A. Bicchi, "Tele-impedance: Teleoperation with impedance regulation using a body–machine interface," *The International Journal of Robotics Research*, vol. 31, no. 13, pp. 1642–1656, 2012.

[15] P. Simoens, M. Dragone, and A. Saffiotti, "The internet of robotic things: A review of concept, added value and applications," *International Journal of Advanced Robotic Systems*, vol. 15, p. 172988141875942, 02 2018.

[16] M. S. Uddin, M. Gianni, and A. Lab, "Long range robot teleoperation system based on internet of things," in *2017 2nd International Conference on Computer and Communication Systems (ICCCS)*, July 2017, pp. 163–167.

[17] F. Ficuciello, L. Villani, and B. Siciliano, "Variable impedance control of redundant manipulators for intuitive human–robot physical interaction," *IEEE Transactions on Robotics*, vol. 31, no. 4, pp. 850–863, 2015.

[18] M. Safeea and P. Neto, "Minimum distance calculation using laser scanner and imus for safe human-robot interaction," *Robotics and Computer-Integrated Manufacturing*, vol. 58, pp. 33–42, 2019.

[19] M. Safeea, P. Neto, and R. Bearee, "On-line collision avoidance for collaborative robot manipulators by adjusting off-line generated paths: An industrial use case," *Robotics and Autonomous Systems*, vol. 119, pp. 278–288, 2019.

[20] H. Su, J. Sandoval, P. Vieyres, G. Poisson, G. Ferrigno, and E. De Momi, "Safety-enhanced collaborative framework for teleoperated minimally invasive surgery using a 7-dof torque-controlled robot," *International Journal of Control, Automation and Systems*, vol. 16, no. 6, pp. 2915–2923, 2018.

[21] B. Horn, "Closed-form solution of absolute orientation using unit quaternions," *Journal of the Optical Society A*, vol. 4, pp. 629–642, 04 1987.

[22] L. A. Groves, P. Carnahan, D. R. Allen, R. Adam, T. Peters, and E. C. S. Chen, "Accuracy assessment for the co-registration between optical and vive head-mounted display tracking," *International Journal of Computer Assisted Radiology and Surgery*, vol. 14, 05 2019.

[23] M. Shimizu, H. Kakuya, W.-K. Yoon, K. Kitagaki, and K. Kosuge, "Analytical inverse kinematic computation for 7-dof redundant manipulators with joint limits and its application to redundancy resolution," *IEEE Transactions on Robotics*, vol. 24, no. 5, pp. 1131–1142, 2008.

[24] L. Zhang, Z. Li, and C. Yang, "Adaptive neural network based variable stiffness control of uncertain robotic systems using disturbance observer," *IEEE Transactions on Industrial Electronics*, vol. 64, no. 3, pp. 2236–2245, March 2017. [Online]. Available: https://ieeexplore.ieee.org/document/7731156

[25] G. Schreiber, A. Stemmer, and R. Bischoff, "The fast research interface for the kuka lightweight robot," in *IEEE Workshop on Innovative Robot Control Architectures for Demanding (Research) Applications How to Modify and Enhance Commercial Controllers (ICRA 2010)*, 2010, pp. 15–21.

[26] S. Garrido-Jurado, R. Muñoz-Salinas, F. J. Madrid-Cuevas, and M. J. Marín-Jiménez, "Automatic generation and detection of highly reliable fiducial markers under occlusion," *Pattern Recognition*, vol. 47, no. 6, pp. 2280–2292, 2014.

[27] H. Su, W. Qi, C. Yang, J. Sandoval, G. Ferrigno, and E. De Momi, "Deep neural network approach in robot tool dynamics identification for bilateral teleoperation," *IEEE Robotics and Automation Letters*, pp. 1–1, 2020.